

Fibroblasts And Mouse's Breast Cancer Cells Can Form Cellular Aggregates in Improved Soft Agar Culture Medium

Xiangnan Zhang

Beijing Niulanshan First Secondary School

Shuo Liang

Beijing Dayu School

Enze Wang

Beijing No.4 High School

Ning Tao (✉ tao@ibp.ac.cn)

Institute of Biophysics, Chinese Academy of Sciences

Research Article

Keywords: Cancer-associated Fibroblast, Breast Cancer Cell, Soft Agar Culture, Cellular Aggregate

Posted Date: April 19th, 2022

DOI: <https://doi.org/10.21203/rs.3.rs-1563613/v1>

License:  This work is licensed under a Creative Commons Attribution 4.0 International License.

[Read Full License](#)

Abstract

Purpose

Cancer-associated fibroblasts (CAFs) promote cancer cell growth, invasion and migration. In this research, we aimed to build cellular aggregates of mouse's breast cancer cells (TS/A) and normal fibroblasts (LX-2) or CAFs (ME-iLX-2) in soft agar culture medium, verifying this co-culture model's value in screening of anticancer drugs and preliminarily demonstrating the effect of CD44 in aggregates formation.

Methods

We improved soft agar culture medium to co-culture CAFs (NFs) and TS/A to build the cellular aggregates model, and compared the amount and area of different co-culture groups. To verify its value in screening of anticancer drugs, eugenol which has been demonstrated its anticancer effect was added into this model. The transcription of human CD44 was analyzed through Real-time quantitative PCR (RT-qPCR).

Result

TS/A-fibroblast cellular aggregates were formed in improved soft agar culture medium. What's more, the amount and area of aggregates in TS/A-ME-iLX-2 co-culture group were significantly higher than in TS/A-LX-2 co-culture group. In co-culture group with eugenol, the amount and area of TS/A-ME-iLX-2 aggregates were lower than control group. The result of RT-qPCR showed that the transcription volume of human CD44 in TS/A-ME-iLX-2 aggregates was higher than in TS/A-LX-2 aggregates.

Conclusion

Co-culturing cellular aggregates of fibroblasts and TS/A was successfully formed in improved soft agar culture medium, and the amount and area of aggregates further confirmed CAFs' promotion effect to cancer cells. Eugenol test showed its value in screening of anticancer drugs. RT-qPCR result demonstrated the important effect of CD44 in aggregates formation.

1 | Introduction

Researches show that, the crosstalk between Cancer-associated fibroblasts (CAFs) and cancer cells promote the cancer process signally[1]. In one hand, CAFs can maintain self-active state by cytokines in autocrine, such as transforming growth factor beta (TGF- β)[2]. In the other hand, CAFs and cancer cells can promote each other by paracrine[3]. In addition, the physical contact between CAFs and cancer cells also promotes the invasion process of cancer cells[4]. In tumor microenvironment (TME), cancer cells promote CAFs secretion of TGF- β by exosomes[5], and CAFs promote the cancer process by the same

way[6]. With no doubt that, the complex crosstalk between CAFs and cancer cells make the building of model in vitro much harder. Some previous researches co-cultured these two cell lines by subcutaneous injection of mice[2], which is difficult to monitor in real time and may cost lots of time to be finished. There are also researchers co-cultured them by conditioned medium[3], but the impact of cell-cell physical contact cannot be reflected in this way. Similarly, in many researches about exosome, researchers extract the exosomes by methods like ultracentrifugation technique and added it into targeted cell lines, but there are problems like too much time cost, low purity and damage of exosomes that may affect the result[7]. By contrast, three-dimensional co-culture can reflect the complex cellular communication fully. Yamaguchi et al. formed large aggregates of scirrhous gastric carcinoma cells and CAFs via three-dimensional Matrigel[8]. Mei et al. built the similar globular structure by breast cancer cells and normal fibroblasts (NFs) on ultra-low adhesion plates[9]. The forming of cellular aggregates is similar to their behavior in vivo[10], which demonstrated the advantage of three-dimensional co-culture in monitoring the crosstalk of CAFs/NFs and cancer cells. However, the problems remain that, they usually cost more and are limited that may not suit CAFs and cancer cells co-culture widely.

The Soft-agar-culture system is a three-dimensional culture method[11]. Because it can better simulate the internal environment of the human body and measure cells transferring capability, it's widely used in researches that have high requirements for cells growth environment, such as the Colony Formation Assay[12] and proliferation and differentiation of spermatogonia stem cells[13]. All that matters is that, the research shows that CAFs can form colonies in soft agar medium because of its high expression of TGF- β [14]. Therefore, we expected to build the co-culture model of CAFs and mouse's breast cancer cells in vitro by Soft-agar-culture system, which can enable us to monitor their crosstalk better.

Eugenol is the active ingredient in cloves which plays a potential role in prevention and alleviation of chronic diseases, especially of cancers[15]. Al-Sharif et al recovered that eugenol can inhibit proliferation of breast cancer cells in many ways and induce apoptosis of breast cancer cells[16]. Moreover, Al-Kharashi et al proved that eugenol suppressed the invasive, migratory and proliferative potential of CAFs as well as paracrine carcinogenesis by regulating the methylation pattern[17]. To verify the screening anticancer drug function of this co-culture model, we added tiny amounts of eugenol and observe its effect to our model.

As a kind of key protein, CD44 on the surface of CAFs promotes drug resistance of cancer cells and maintains the stemness of cancer cells[18]. Sharma et al. demonstrated that, CD44 might be an important mediator of heterotypic clustering of CAFs and breast cancer cells[10]. To explore the mechanism and CD44's effect of cellular aggregates formation, we analyzed the transcription volume of CD44 through Real-time quantitative PCR (RT-qPCR).

2 | Materials And Methods

2.1 | Cell Culture

TS/A cell line was built by Nanni et al. in 1983, which has been described previously[19]. TS/A in this research is provided by Zhihai Qin Research Group, Institute of Biophysics, Chinese Academy of Sciences. ME-iLX-2 cell line were the LX-2 cell line which was induced by TS/A cells supernatant for 43 days to obtain the characteristics of CAFs, provided by Enze Wang (data not shown). These two cell lines is stored in Dulbecco's Modified Eagle's Medium (HyClone, USA) which has been added with 10% fetal bovine serum (PAN, Germany) and 1% penicillin-streptomycin. All the cells are placed in 37°C/ 5%CO₂ constant temperature incubator.

2.2 | Soft-agar Culture

We prepared the soft agar culture medium according to the protocol by Borowicz et al[20]. To improve the stability, we raised the concentration of low-temperature agarose to 0.4% and 0.6% in upper and lower layers. The low-temperature agarose was purchased from Sigma-Aldrich, USA. The co-culture was proceeded in 6-well culture plate. To reduce cell adherence, we placed two layers of agar gel. The volume of each layer was 1.5mL and only upper layer was mixed with cells. In addition, as for the long-time culture, we added 100μL well-prepared DMEM each well on the surface of gels ever three days, so that they can maintain wet and well-nurished.

Data was collected via phase contrast microscope photography and a Canon SLR at the location of highest cell density in each well. ImageJ procedure is used to analyze the number and area of aggregates from images. Adobe Photoshop 2021 is used to adjust images' color, brightness contrast, etc. to make images clearer, and cut out and splice them in suitable size. Graphs were made by GraphPad Prism 6.

2.3 | Eugenol Inhibition of Aggregates

Eugenol in this research is purchased from Beijing Beina Chuanglian Biotechnology Institute, China. The soft-agar culture method is the same as 2.2. A total of 1.5×10^5 TS/A cells and ME-iLX-2 cells were inoculated in each well with a ratio of 1:9. 2μL eugenol(6000 mmol/mL, 99.3%) and 198μL well-prepared DMEM for each well are mixed in advance. The mixture was added after the agar gel is solidify in the room temperature. We placed the culture system into 37°C/ 5%CO₂ constant temperature incubator and collected the data after three days.

2.4 | Real-time quantitative PCR (RT-qPCR)

2.4.1 | RNA Extraction and Reverse Transcription PCR

To separate cellular aggregates and soft agar culture medium, the culture system was firstly added DMEM culture medium which had been warmed at 37°C, then the soft agar was smashed and placed in a 15mL centrifugal tube. The smashed soft agar was heated at 42°C for 30 minute until be melted. After that, the tube was centrifuged at 1200 RPM for 10 minutes. The supernatant was discarded and 500mL TRIzol (Sigma, USA) was added to make cells lytic. The extracted RNA solution's concentration and purity were confirmed by Ultramicro photometer (NanoDrop Technologies, Wilmington, DE, USA). Reverse

transcription PCR was conducted with RT-PCR kit (Abcam, UK) and its program was set as “37°C, 15min;85°C, 5s;4°C, ∞”. The acquired cDNA was stored in -40°C refrigerator.

2.4.2 | RT-qPCR

The 20μL reaction system was compounded by RT-qPCR kit (GenStar, USA) and was shortly stored in 4°C refrigerator. Firstly predegeneration was conducted via program as “95°C, 90s”, then the program was set as “95°C, 10s;60°C, 30s;72°C, 20s” and repeated for 40 times. The specific primer of human gapdh (as internal reference) and human cd44 are as followed: gapdh forward 5'-CTGGGCTACACTGAGCACC-3' and reverse 5'-AAGTGGTCGTTGAGGGCAATG-3'; cd44 forward 5'-CTGCCGCTTTGCAGGTGTA-3' and reverse 5'-CATTGTGGGCAAGGTGCTATT-3'. CD44 RNA content was calculated by $2^{-\Delta\Delta CT}$ Method.

3 | Result

3.1 | Cellular Aggregates Can Form in Soft Agar Culture Medium

We co-cultured TS/A-ME-iLX-2 and TS/A-LX-2 in the soft agar culture medium for 7 days, and cultured TS/A, ME-iLX-2 and LX-2 separately in the same time. In the co-culture systems, A total of 1.5×10^5 TS/A and fibroblasts were inoculated in each well with a ratio of 1:9. In the separating culture system, the number of TS/A in each well was 1.5×10^4 , both of the numbers of ME-iLX-2 and LX-2 in each well were 1.35×10^5 . The morphological characteristics of cellular aggregates are as *Fig. 1a*. We select three pictures of aggregates in each group to comprehensively reflect their morphology. In order to improve the sharpness of the image, this image is set to grayscale mode and the image contrast is improved. This figure does not retain the original size relation of aggregates when stitching.

After 3 days, we discovered the aggregates in two co-culture systems and ME-iLX-2 and LX-2. In the following days, TS/A-ME-iLX-2 aggregates didn't change visibly. TS/A-LX-2 Aggregates are formed by vesicular secondary structures in the third and fourth day, and then changed into the pyknotic globular structures which is similar as TS/A-ME-iLX-2 aggregates. The aggregates of ME-iLX-2 and LX-2 changed little, but some of them formed the globular structures in the fifth day. In the seventh day, aggregates of these two cell lines still presented large loose vesicular structures, but they were more pyknotic than before, which showed that they have the potential to form the globular structures. On the whole, aggregates of the co-culture systems were clear in shape, smooth in contour and compact in structure. The other two systems were in the opposite and usually formed by vesicular secondary structures. It's worth noting that, comparing the aggregates of TS/A-ME-iLX-2 and TS/A-LX-2 in the third and fourth day, we discovered that TS/A-ME-iLX-2 system formed the pyknotic globular structure earlier than TS/A-LX-2 system, which showed ME-iLX-2's auxo-action for formation of the aggregates.

In fact, in the separating culture system of TS/A, we also discovered the cell aggregation. However, to be compared with the above-mentioned systems, the morphological characteristics of TS/A aggregates were

not specific, and have tiny areas through microscope. In the seventh day, we discovered a macroscopical colony of TS/A as *Fig. 1b*, which didn't appear in other systems.

3.2 | ME-iLX-2 Promotes Formation of Cellular Aggregates

To reveal the ME-iLX-2's promotion in cellular aggregates formation, we counted the number and area of aggregates in each group. The results are shown in *Fig. 2b* and *c*. In the five groups, TS/A + ME-iLX-2 group had the largest aggregate quantity and area. The difference between TS/A + ME-iLX-2 group and TS/A + LX-2 group is significant. *Figure 2c* illustrates that, the total area of TS/A-ME-iLX-2 aggregates generally increased, and the growth rate slowed down gradually. According to *Fig. 2d*, the area of TS/A-LX-2 increased from the third day to the sixth day. The maximum appeared on the third day, and the minimum appeared on the sixth day. In conclusion, ME-iLX-2 has a stronger promoting effect on cellular aggregates formation than LX-2.

Taking into the consideration that there is a complex crosstalk between TS/A and ME-iLX-2 in co-culture, which cannot happen in separating culture, we counted the sum of aggregates' amount in co-culture and separating culture to reveal the influence of crosstalk between TS/A and ME-iLX-2 on aggregate formation. The result is shown on *Fig. 2e*. The amount in co-culture group is significantly higher than in separating culture group ($p < 0.01$), which strongly demonstrated the promoting effect of the crosstalk between TS/A and ME-iLX-2 in aggregate formation and the advantage of co-culture model.

3.3 | Eugenol Inhibits TS/A-ME-iLX-2 Aggregates

We conducted the experiment as 2.3. The image results are shown on *Fig. 3c*. According to these images, the aggregates in the control group was full in shape, while the aggregates in the experimental group seemed to atrophy. We counted the amount and area of two groups after three day's culture, which are shown on *Fig. 3a b*. Both the amount and the area in the experimental group are significantly lower than the control group ($p < 0.05$). This experiment proved the inhibition of Eugenol on TS/A-ME-iLX-2 aggregates formation.

3.4 | CD44 Is Highly Expressed in ME-iLX-2 from TS/A-ME-iLX-2 Aggregates

To explore the possible mechanism of ME-iLX-2's promotion to cellular aggregates formation, human CD44 transcription RNA volume of TS/A-LX-2 aggregates and TS/A-ME-iLX-2 aggregates at 3 to 4 days were analysis by RT-qPCR. The result is as *Fig. 4c*. Data shows that, CD44 transcription volume of TS/A-ME-iLX-2 aggregates is significantly higher than of TS/A-LX-2 aggregates ($p \ll 0.01$). Based on the research by Sharma et al., it is possible that ME-iLX-2 increases the expression of CD44 to enhance its ability to attract TS/A together, which can improve the amount and area of TS/A-ME-iLX-2 aggregates.

4 | Discussion

Undoubtedly, monitoring the crosstalk between cancer cells and CAFs in vitro will provide great help for the research of tumor microenvironment and the screening of related anticancer drugs. In this research, we built a model in vitro, which can reflect the crosstalk between cancer cells and fibroblasts via cellular aggregates. To compare with the traditional methods that researching cancer cells and CAFs separately, this co-culture enables researchers to research cancer cells and CAFs as a whole, which could be a very interesting research perspective. In addition, to compare with the methods like subcutaneous injection of mice, co-culture in soft agar culture medium enables researchers to monitor cellular aggregates' growth and progress so that they can gain more detailed information about cancer process. In practice, the co-culture method is simple, convenient and timesaving, which can reduce the cost for researchers.

In the aggregate formation experiment, we speculate that the reason why the TS/A-ME-iLX-2 aggregates presented the above area trend (Fig. 2c) is that the nutrients are gradually consumed, or ME-iLX-2 was inferior in the nutritional competition between TS/A and ME-iLX-2 which may cause the decreasing of promoting aggregates formation. The decrease of area on the sixth day may be mainly due to the lack of nutrients in the system. We added DMEM on the sixth day, which can explain the increasing from the sixth day to the seventh day. According to above-mentioned information, we conjectured that the nutrient requirement of TS/A-ME-iLX-2 aggregates is more than of TS/A-LX-2 aggregates. Moreover, the areas of TS/A-ME-iLX-2 aggregates are larger than the areas of TS/A-LX-2 aggregates on the same day. In conclusion, we speculate that ME-iLX-2 provide a better environment to aggregate formation.

In eugenol inhibition of aggregates, considering the differences of the quantity, area and morphology of cell aggregates, we believe that this inhibition may occur in two ways: 1. Eugenol inhibits the cellular aggregation which can decrease the number of cellular aggregates. 2. Eugenol inhibits the growth of cellular aggregates after its formation. The differences between control group and experimental group demonstrated eugenol's inhibition of the aggressive structure of cancer in vitro as well as this soft agar co-culture model's function of anticancer drug screening.

As for the mechanism of the aggregate's formation, Sharma et al pointed out that CD44 may be the medium between CAFs and cancer cells[10]. Yamaguchi et al. pointed out that this behavior may be related to the activation of intracellular signaling pathways that regulate actomyosin contractility[8]. Based on the research by Sharma et al., we found that CD44 expression is significantly higher in TS/A-ME-iLX-2 aggregates than in TS/A-LX-2 aggregates, which not only confirms perspective of Sharma et al, but also can be used to refer that, as CAFs, ME-iLX-2 enhance its expression of CD44 to improve its ability to attract TS/A together, which can be a reason why the amount and area of TS/A-ME-iLX-2 aggregates are higher(Fig. 5). In addition, it is also a possible way to increase the amount and area of TS/A-ME-iLX-2 aggregates that CAFs promote the propagation of cancer cells in many ways.

Actually, the composition of the tumor microenvironment is quite complex. Not only does it includes CAFs which is researched in this research, but also includes endothelial cells, mesenchymal stem cells (MSCs), immune cells and even vascular, lymphatic network, etc.[21]. Though the soft-agar co-culture can simulate the crosstalk between cancer cells and CAFs, the capability of its simulated tumor

microenvironment needs to be further studied. Considering that MSCs have the ability to recruit and differentiate into CAFs[22], and CAFs can also recruit MSCs[23], we speculate that MSCs can promote cellular communication in this soft-agar model. What's more, biophysical interactions in tumor microenvironment also promote the metastasis of cancer cells[24]. It is also need to be further studied that how to simulate the chemical and mechanical signals better.

In this research, we counted aggregates' amount and area to reflect their formation and growth, because there were great morphological differences among the cell aggregates, which is particularly significant between the co-culture system and separated fibroblasts. However, it also leads to the problem that the amount and area are always inevitably different when we make statistics. There is still a lack of more scientific indicators and algorithms to make a more accurate assessment of cellular aggregates.

Declarations

Acknowledgements

We are grateful to *The science & Technology Training Program for Adolescents in Beijing* for its financial support.

References

1. Hurtado P,Martínez-Pena I,Piñeiro R (2020) Dangerous Liaisons: Circulating Tumor Cells (CTCs) and Cancer-Associated Fibroblasts (CAFs). *Cancers (Basel)*. 12(10).<https://doi.org/10.3390/cancers12102861>
2. Kojima Y,Acar A,Eaton EN,Mellody KT,Scheel C,Ben-Porath I,Onder TT,Wang ZC,Richardson AL,Weinberg RA,Orimo A (2010) Autocrine TGF-beta and stromal cell-derived factor-1 (SDF-1) signaling drives the evolution of tumor-promoting mammary stromal myofibroblasts. *Proc Natl Acad Sci U S A*. 107(46):20009–14.<https://doi.org/10.1073/pnas.1013805107>
3. Awaji M,Saxena S,Wu L,Prajapati DR,Purohit A,Varney ML,Kumar S,Rachagani S,Ly QP,Jain M,Batra SK,Singh RK (2020) CXCR2 signaling promotes secretory cancer-associated fibroblasts in pancreatic ductal adenocarcinoma. *Faseb j*. 34(7):9405–9418.<https://doi.org/10.1096/fj.201902990R>
4. Yamaguchi H,Sakai R (2015) Direct Interaction between Carcinoma Cells and Cancer Associated Fibroblasts for the Regulation of Cancer Invasion. *Cancers (Basel)*. 7(4):2054–62.<https://doi.org/10.3390/cancers7040876>
5. Dai G,Yao X,Zhang Y,Gu J,Geng Y,Xue F,Zhang J (2018) Colorectal cancer cell-derived exosomes containing miR-10b regulate fibroblast cells via the PI3K/Akt pathway. *Bull Cancer*. 105(4):336–349.<https://doi.org/10.1016/j.bulcan.2017.12.009>
6. Sansone P,Savini C,Kurelac I,Chang Q,Amato LB,Strillacchi A,Stepanova A,Iommarini L,Mastroleo C,Daly L,Galkin A,Thakur BK,Soplop N,Uryu K,Hoshino A,Norton L,Bonafé M,Cricca M,Gasparre G,Lyden D,Bromberg J (2017) Packaging and transfer of mitochondrial DNA via exosomes regulate

- escape from dormancy in hormonal therapy-resistant breast cancer. *Proc Natl Acad Sci U S A*. 114(43):E9066-e9075.<https://doi.org/10.1073/pnas.1704862114>
7. Zhu L, Sun HT, Wang S, Huang SL, Zheng Y, Wang CQ, Hu BY, Qin W, Zou TT, Fu Y, Shen XT, Zhu WW, Geng Y, Lu L, Jia HL, Qin LX, Dong QZ (2020) Isolation and characterization of exosomes for cancer research. *J Hematol Oncol*. 13(1):152.<https://doi.org/10.1186/s13045-020-00987-y>
 8. Yamaguchi H, Yoshida N, Takanashi M, Ito Y, Fukami K, Yanagihara K, Yashiro M, Sakai R (2014) Stromal fibroblasts mediate extracellular matrix remodeling and invasion of scirrhous gastric carcinoma cells. *PLoS One*. 9(1):e85485.<https://doi.org/10.1371/journal.pone.0085485>
 9. Mei J, Böhländ C, Geiger A, Baur I, Berner K, Heuer S, Liu X, Mataite L, Melo-Narváez MC, Özkaya E, Rupp A, Siebenwirth C, Thoma F, Kling MF, Friedl AA (2021) Development of a model for fibroblast-led collective migration from breast cancer cell spheroids to study radiation effects on invasiveness. *Radiat Oncol*. 16(1):159.<https://doi.org/10.1186/s13014-021-01883-6>
 10. Sharma U, Medina-Saenz K, Miller PC, Troness B, Spartz A, Sandoval-Leon A, Parke DN, Seagroves TN, Lippman ME, El-Ashry D (2021) Heterotypic clustering of circulating tumor cells and circulating cancer-associated fibroblasts facilitates breast cancer metastasis. *Breast Cancer Res Treat*.<https://doi.org/10.1007/s10549-021-06299-0>
 11. Stukenborg JB, Wistuba J, Luetjens CM, Elhija MA, Huleihel M, Lunenfeld E, Gromoll J, Nieschlag E, Schlatt S (2008) Coculture of spermatogonia with somatic cells in a novel three-dimensional soft-agar-culture-system. *J Androl*. 29(3):312 – 29.<https://doi.org/10.2164/jandrol.107.002857>
 12. Horibata S, Vo TV, Subramanian V, Thompson PR, Coonrod SA (2015) Utilization of the Soft Agar Colony Formation Assay to Identify Inhibitors of Tumorigenicity in Breast Cancer Cells. *J Vis Exp*. 99):e52727.<https://doi.org/10.3791/52727>
 13. Mohammadzadeh E, Mirzapour T, Nowroozi MR, Nazarian H, Piryaee A, Alipour F, Modarres Mousavi SM, Ghaffari Novin M (2019) Differentiation of spermatogonial stem cells by soft agar three-dimensional culture system. *Artif Cells Nanomed Biotechnol*. 47(1):1772–1781.<https://doi.org/10.1080/21691401.2019.1575230>
 14. San Francisco IF, DeWolf WC, Peehl DM, Olumi AF (2004) Expression of transforming growth factor-beta 1 and growth in soft agar differentiate prostate carcinoma-associated fibroblasts from normal prostate fibroblasts. *Int J Cancer*. 112(2):213–8.<https://doi.org/10.1002/ijc.20388>
 15. Fujisawa S, Murakami Y (2016) Eugenol and Its Role in Chronic Diseases. *Adv Exp Med Biol*. 929(45–66).https://doi.org/10.1007/978-3-319-41342-6_3
 16. Al-Sharif I, Remmal A, Aboussekhra A (2013) Eugenol triggers apoptosis in breast cancer cells through E2F1/survivin down-regulation. *BMC Cancer*. 13(600).<https://doi.org/10.1186/1471-2407-13-600>
 17. Al-Kharashi LA, Bakheet T, AlHarbi WA, Al-Moghrabi N, Aboussekhra A (2021) Eugenol modulates genomic methylation and inactivates breast cancer-associated fibroblasts through E2F1-dependent downregulation of DNMT1/DNMT3A. *Mol Carcinog*.<https://doi.org/10.1002/mc.23344>
 18. Kinugasa Y, Matsui T, Takakura N (2014) CD44 expressed on cancer-associated fibroblasts is a functional molecule supporting the stemness and drug resistance of malignant cancer cells in the

- tumor microenvironment. *Stem cells* (Dayton, Ohio). 32(1):145 – 56.<https://doi.org/10.1002/stem.1556>
19. Nanni P, de Giovanni C, Lollini PL, Nicoletti G, Prodi G (1983) TS/A: a new metastasizing cell line from a BALB/c spontaneous mammary adenocarcinoma. *Clin Exp Metastasis*. 1(4):373 – 80.<https://doi.org/10.1007/BF00121199>
 20. Borowicz S, Van Scoyk M, Avasarala S, Karuppusamy Rathinam MK, Tauler J, Bikkavilli RK, Winn RA (2014) The soft agar colony formation assay. *J Vis Exp*. 92):e51998.<https://doi.org/10.3791/51998>
 21. Wei R, Liu S, Zhang S, Min L, Zhu S (2020) Cellular and Extracellular Components in Tumor Microenvironment and Their Application in Early Diagnosis of Cancers. *Anal Cell Pathol (Amst)*. 2020(6283796).<https://doi.org/10.1155/2020/6283796>
 22. Quante M, Tu SP, Tomita H, Gonda T, Wang SS, Takashi S, Baik GH, Shibata W, Diprete B, Betz KS, Friedman R, Varro A, Tycko B, Wang TC (2011) Bone marrow-derived myofibroblasts contribute to the mesenchymal stem cell niche and promote tumor growth. *Cancer Cell*. 19(2):257 – 72.<https://doi.org/10.1016/j.ccr.2011.01.020>
 23. Orimo A, Gupta PB, Sgroi DC, Arenzana-Seisdedos F, Delaunay T, Naeem R, Carey VJ, Richardson AL, Weinberg RA (2005) Stromal fibroblasts present in invasive human breast carcinomas promote tumor growth and angiogenesis through elevated SDF-1/CXCL12 secretion. *Cell*. 121(3):335 – 48.<https://doi.org/10.1016/j.cell.2005.02.034>
 24. Vasilaki D, Bakopoulou A, Tsouknidas A, Johnstone E, Michalakis K (2021) Biophysical interactions between components of the tumor microenvironment promote metastasis. *Biophys Rev*. 13(3):339–357.<https://doi.org/10.1007/s12551-021-00811-y>

Figures

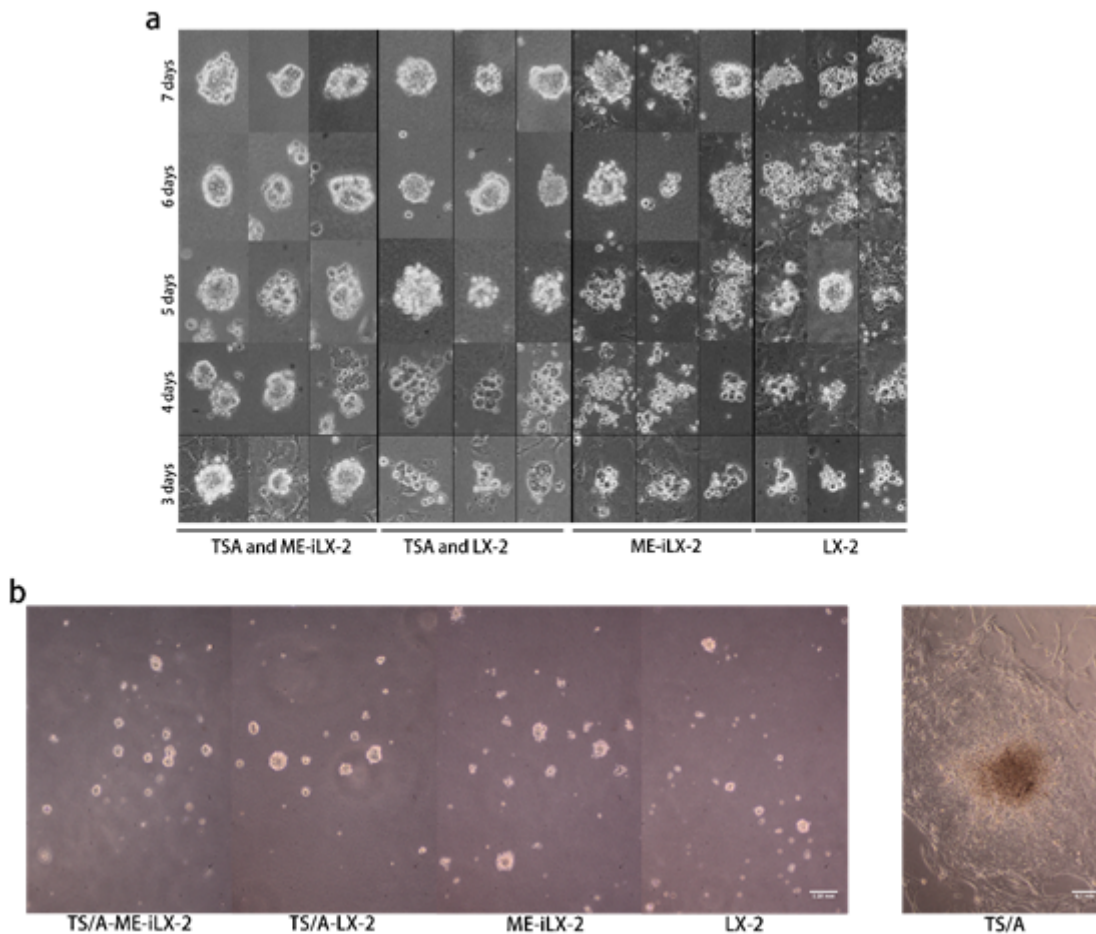


Figure 1

Cellular Aggregates and Colony in Soft Agar Culture System **a** Morphology of co-culture TS/A and ME-iLX-2, co-cultured TS/A and LX-2, separated ME-iLX-2 and separated LX-2 **b** 7 days culture systems images under microscope.

Figure 2

Amount and Area of TS/A-ME-iLX-2 and TS/A-LX-2 Cellular Aggregates **a** The Area of aggregates in each group ($P < 0.05$ between TS/A+ME-iLX-2 and TS/A+LX-2 group) **b** The number of cellular aggregates in each group after three days ($P < 0.01$ between TS/A+ME-iLX-2 and TS/A+LX-2 group) **c** Changes in the mean of the area of TS/A-ME-iLX-2 aggregates over time from third to seventh day ($P < 0.05$ between the maximum and the minimum) **d** Changes in the mean of the area of TS/A-LX-2 aggregates over time from third to seventh day ($P < 0.05$ between the maximum and the minimum) **e** The number of aggregates of co-cultured and separated TS/A and ME-iLX-2 ($P < 0.01$)

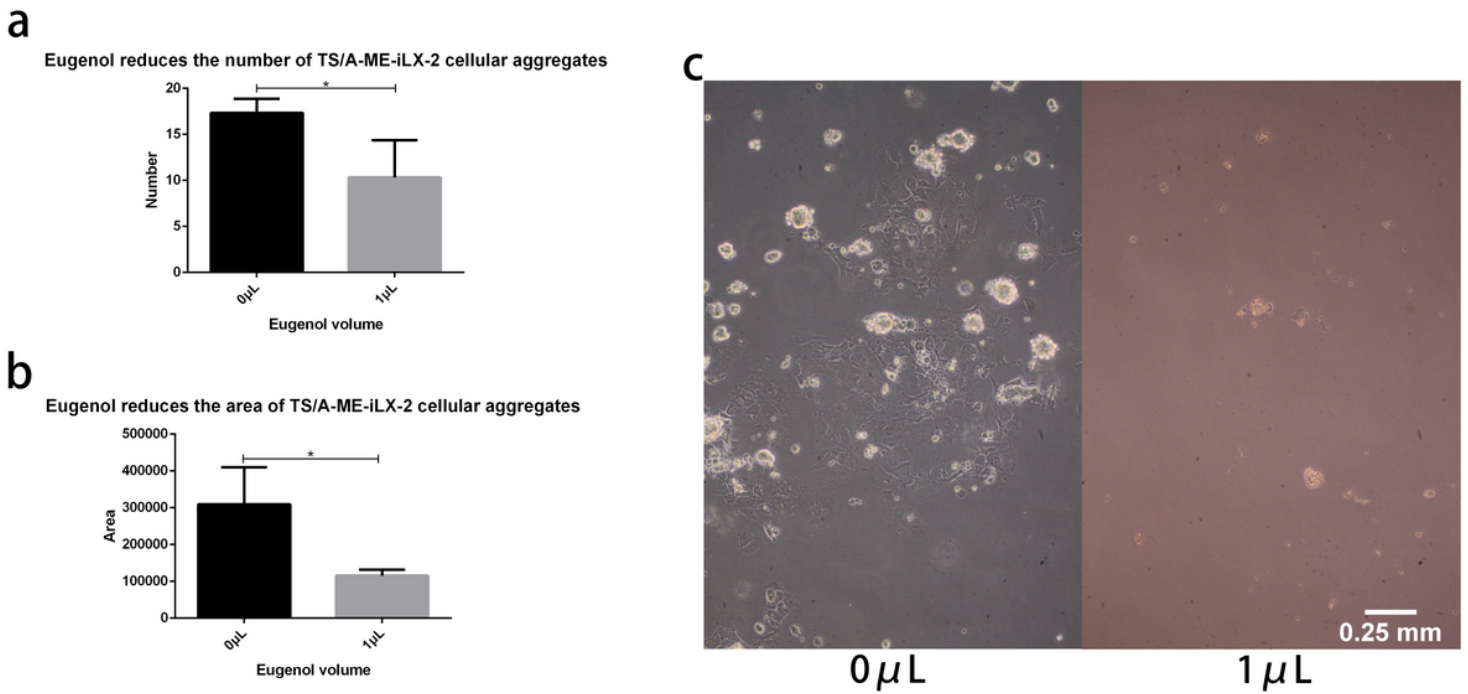


Figure 3

Eugenol Inhibits the Formation of TS/A-ME-iLX-2 Cellular Aggregates **a** Eugenol decrease the number of TS/A-ME-iLX-2 aggregates ($P < 0.05$) **b** Eugenol reduce the area of TS/A-ME-iLX-2 aggregates ($P < 0.05$) **c** The effect of eugenol on TS/A-ME-iLX-2 aggregates' Morphology, expanded for 100 times.

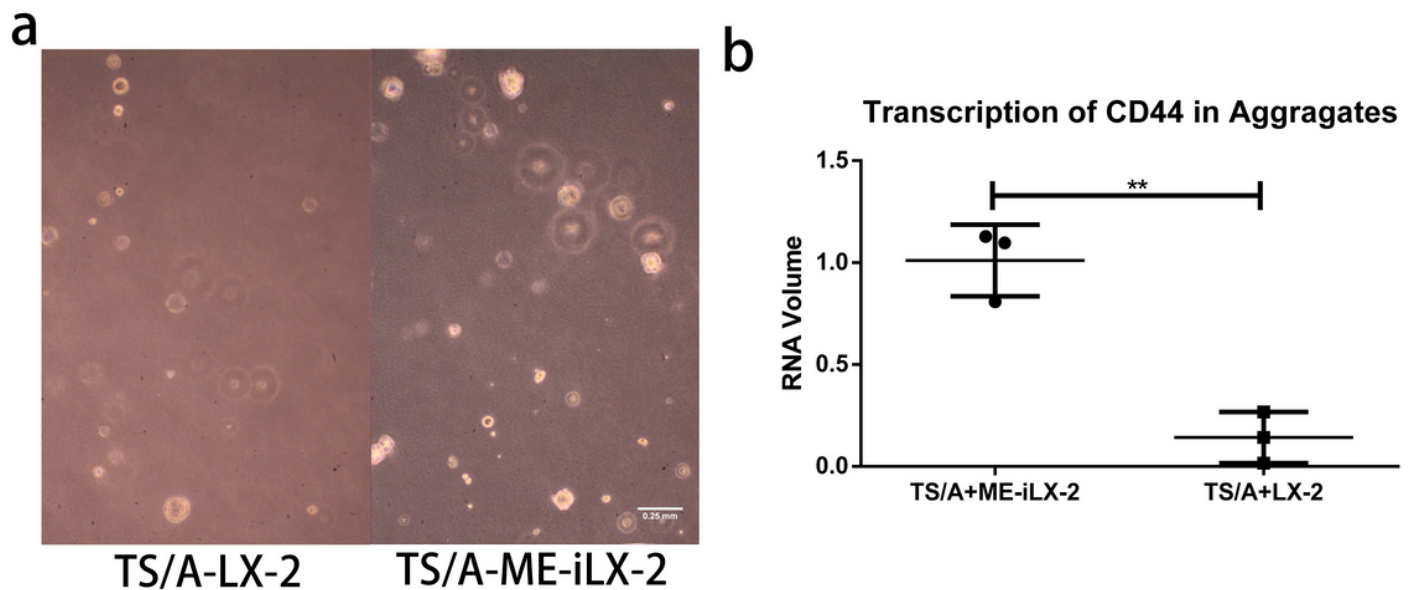


Figure 4

RT-qPCR Result of Transcription of CD44 in Cellular Aggregates **a** TS/A-LX-2 aggregates and TS/A-ME-iLX-2 aggregates at 3 to 4 days, expanded for 100 times **b** Human CD44 transcription RNA volume in TS/A-ME-iLX-2 and TS/A-LX-2 aggregates, calculated by $2^{-\Delta\Delta CT}$ $p < 0.01$

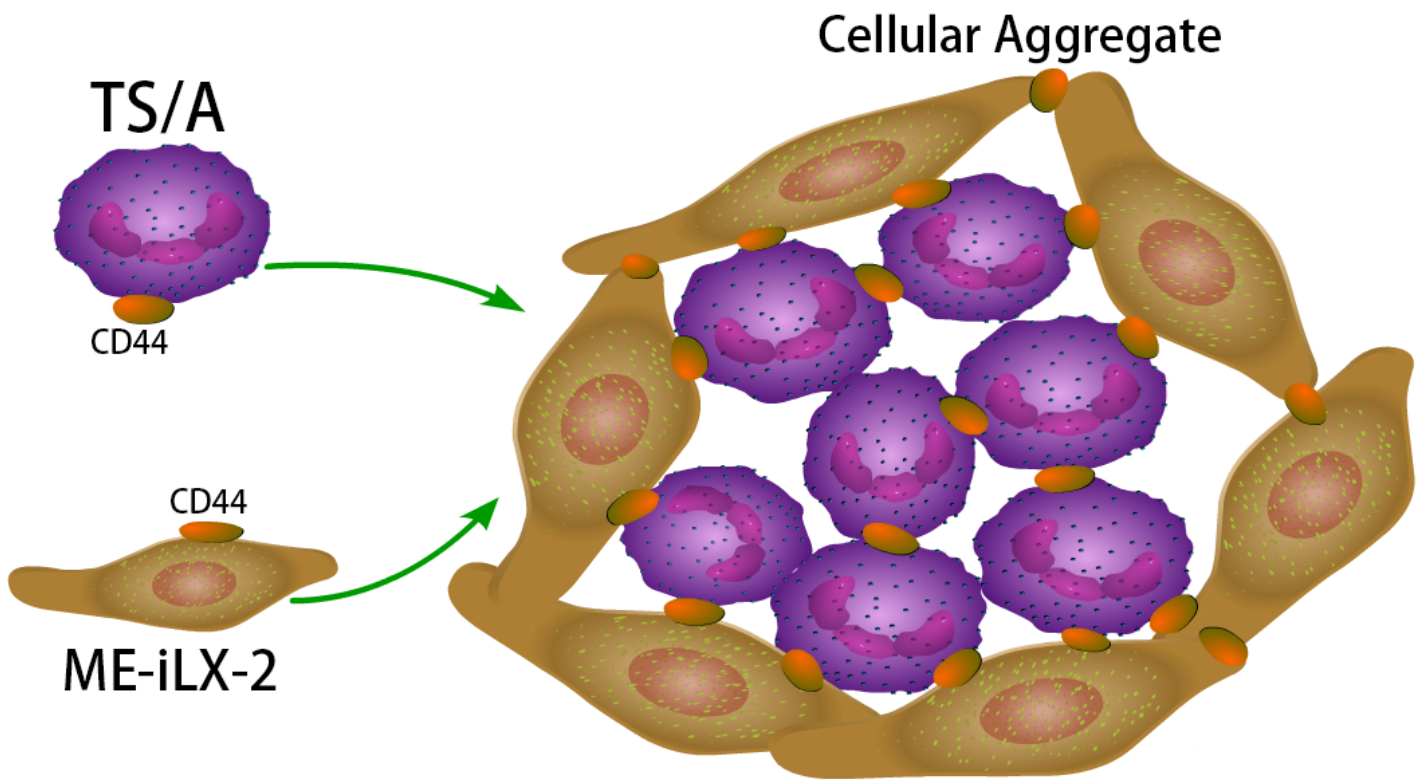


Figure 5

Possible Formation Mechanism of TS/A-ME-iLX-2 Cellular Aggregates